Performance Evaluation of a Mini–Vertical Axis Cross Flow Helical Turbine Meant for Energy Extraction from Dam's Tailrace

V. Jayaram*‡, B. Bavanish**, Mohammed Fahad *** P. A. Azeem Hafiz ****,

Niaz A. Salam*****

* Assistant professor, Department of Mechanical Engineering, Lourdes Matha college of science and Technology, Kuttichal, Trivandrum -Kerala India

** Principal, Noorul Islam College of Engineering and Technology, Pookadai,Thiruvithancode, Kanyakumari district, Tamilnadu India

*** Department of Mechanical Engineering, Muslim Association college of engineering, Venjaramoodu, Trivandrum -Kerala India

**** Principal, Travancore Engineering College, Oyoor, Kollam, Kerala, India

*****Research Scholar, Department of Mechanical Engineering, College of Engineering Trivandrum, Kerala, India

(jayaramvijayan@gmail.com, dr.bbavanish@gmail.com, Mohammedfahadphd@gmail.com, azeemparayil@gmail.com, niazasalam@gmail.com)

‡ Assistant Professor, LMCST, Trivandrum Kerala India Tel: +90 9809816191, jayaram.v@lmcst.ac.in

Received: 19.06.2023 Accepted:20.08.2023

Abstract- Research targeting renewable energy harnessing has gained considerable momentum in the past decade, given the decreasing status of fossil fuel reserves. Hydropower generates constitutes the lion's share of renewable energy worldwide. However, they continue to be underutilized. Hydropower generation from tailrace water offers significant prospects for micro-hydro power generation, which, if effectively implemented, can help improve a power grid's rating. The primary purpose of this investigation is to determine the viability of vertical axis cross-flow turbines with helical blades for deployment in such settings. Solidworks was used to model the Gorlov Helical Turbine. The Gorlov Helical Turbine model is simulated using Ansys Fluent. The principal objective is to determine the turbine's performance at a velocity of 2.54 m/s. NACA 4412 was chosen as the helical blade's aerofoil. The study is validated by experimentation using a 3D printed model. According to the simulation and experiment, the power (output) of GH was 1.78 W and 1.24 W, respectively. The turbine's performance was adequate for deployment based on output power Vs tip speed ratio plots. The result substantiates the studies on the effective integration of cross-flow turbines in the tail race of a dam to increase the grid efficiency of Small Hydro Projects.

Keywords Gorlov Helical Turbine (GHT), Dynamic mesh, 6 DOF (Degree of Freedom), 3D Printing, Experimentation.

1. Introduction

Conventional energy sources are racing against the clock, and the utilization of renewable energy sources is a matter of utmost implication importance. Current restructurings by NITI Ayog (India's government's policy committee) have upgraded noticeably by establishing and proposing a sole nationwide power system driven by advanced thermal and renewable systems. The energy sector in India is currently undergoing a substantial shift towards greater proportions of renewable energy, highlighting the critical importance of system integration and flexibility. The current government is constantly working towards the complete electrification of the country and has fruitfully accomplished bringing power to more than 700 million people since 2000. India intends to have 175 GW of renewable energy deployed by the end of 2023, out of which 5 GW is from small hydropower energy. Grid-connected renewable energy potential touched 84 GW at the end of November 2020, with 32 GW from solar photovoltaic, about 37 GW from onshore wind and the remainder from small hydro. The estimate of renewable energy in India by source

as of 2020 is depicted in Figure 1. Small hydel power plants have a capacity of less than or equal to 2 MW but greater than or equal to 25 MW. As per Indian standards, micro hydel power plants in India are those with a capacity of less than or equal to 100 kW. Hydropower stands as the most extensively utilized renewable energy source on our planet. Unlike outmoded power stations that use fossil fuels like coal or crude oil, hydroelectric power does not contaminate the environment. Researchers and academicians are constantly involved in the experimentation and analysis to make water turbines more efficient [1]. Traditional turbines excel at the higher discharge-lower head and lower discharge-higher head applications. In ultra-low head applications, however, they are nearly outdated. If properly implemented, the hydropower from tailrace water offers appealing prospects for mini/micro hydropower generation, which can raise the rating of a power grid. Unfortunately, the hydropower potential of such a plan is frequently disregarded because it is thought to be unprofitable.

Cross-flow turbines are best suited for such purposes. The water travels across the turbine blades in a cross-flow turbine instead of passing through the turbine axially or radially. The Gorlov helical turbine (GHT) is a vertical axis cross-flow helical-bladed water turbine originating from the Darrieus turbine. The article stresses the performance evaluation of GHT and how it helps extract hydel power for Small Hydro Power plants (SHP). It is also possible to employ barriers against an unrestricted flow, thereby making the system dam-free. These barriers can provide a low-head without obstructing fish passage through the turbines. The GHT is known to self-start at low currents and can rotate even when the course of the current changes, making the turbine preferred for low-head options. Gorlov's [2] initial studies were based on 3 bladed helical turbines (0.6 m in diameter and 0.86 m in height). Gorlov used a NACA0020 aerofoil with a 0.1778 m chord for stability, achieving 35% efficiency. Shiono et.al. [3] took a different approach to GHT design. Shiono tested four models of GHT, all with a 300 mm diameter and height. Each turbine had a different solidity ratio (0.20 to 0.50 in increments of 0.1). He found that the helical blade turbines exhibited fewer pulsation and better starting characteristics than straight blade turbines. Solidity significantly influenced starting, while blade angle did not. The experimental results suggested an optimal solidity ratio of 0.4. Pongduang et al. [4] performed an experimental study into the efficiency and characteristics of GHT subjected to a variable angle of twist. They developed two scaled models with diameters of 0.5 m and 0.6 m (the height of both models was 1.25 m). They chose the NACA0020 symmetric blade profile with a 0.07 m chord length. The best results were obtained for a GHT with a helix angle of 135◦ and a Tip Speed Ratio ranging from 2.2 to 2.5.

Dams meant for irrigation and drinking water supply have a tailrace to drain out the excess amount of water from the reservoir. Similarly, the hydropower plant is equipped with the same tailrace that connects the outflow of the turbine to the downstream side of the river system. Liu & Packey [5] explored the viability and potential of enhancing hydropower generation through a proposed model called a "combined cycle hydropower system". The model was similar to the one discussed above. However, the practical aspects were not studied. Later a broader aspect of the same was assessed by Quaranta & Muntean [6] from the European geographical perspective. Quaranta & Muntean [6] suggested that energy could be harnessed by installing hydrokinetic turbines on the downstream side of the draft tube outlet.

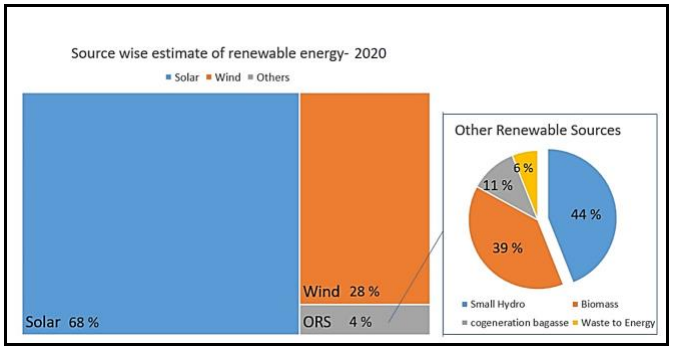

Fig. 1. Source wise estimate of renewable energy of India as of 2020.

Arango [7] in his thesis for master's, evaluated the resource assessment and feasibility study for using hydrokinetic turbines in the tailrace of the Wanapum dam (part of the Columbia River system). Commercial turbines such as the EnCurrent turbine with a capacity of 25 KW for a flow velocity of 1.75 to 2.5 m/s were realised for the project. However, the extent of physical realisation is not known. Most researchers tend to propose a methodology for energy extraction from the tailrace. However, in the current research, the methodology is backed by simulation and laboratory experimentation. For the Uldolmok Strait in South Korea, Gorlov [8] proposed a full-scale floating tidal power station with vertical triple-helix turbines. Only a twin-turbine system is still in use, though. The design and analysis of using ultra-low head microturbines to extract energy from the dam's tail race has not been investigated thoroughly and systematically. Thus, the current research introduces a novel approach to the same.

The Aruvikkara dam's (Kerala, India) reservoir receives water from the Peppara dam. This gravity-masonry dam spans the Karamana River and is utilized to irrigate and deliver drinking water to Thiruvananthapuram city. The span of the dam is 83 m, and its height is 14 m. There are six spillway shutters on the dam to regulate the water flow downstream. On an average day, two of them would be open. The volume flow is so arranged that while rising the shutter by 10 cm, 6 m^3/s of water would flow through it. A test section was identified where the GHT could be installed in arrays. The test section where the turbine is to be deployed is 75 m wide and 2 m deep. The section considered is 45 m downstream from the shutter gates. The turbulence is expected to reduce at this distance. The water flows with a velocity of 2.54 m/s at the test section. Physical measurements were made to confirm the Kerala Water Authority (KWA) data. A GHT is modelled using Solidworks and analysed using a Fluent solver in Ansys. Then the model is printed using a 3D printer. A lab testing of the model for performance evaluation is conducted for the viability of installation on site. A proposed micropower unit is illustrated in Figure 2.

The specific objectives of the work are listed below.

- Propose a methodology to extract energy from the tail race of a dam using an ultra-low head cross-flow turbine (GHT)- Assessment of resource requirement for the power plant and design of such a system.

- Design a single module of GHT and model it using commercially available software (SolidWorks) and simulate the model in the exact environment of the tailrace (flow velocity=2.54 m/s).

- 3D Print the model and evaluate it experimentally under the same environment as that of the tailrace (flow velocity=2.54 m/s). The findings of simulation and experimentation are carefully evaluated.

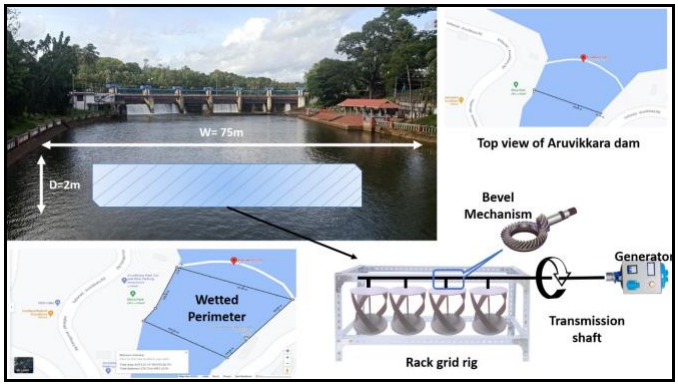

Fig. 2. Proposed micropower generation system using GHT.

2. Design Methodology

The hydropower capacity lies not only in large basins but also in vast oceans and streams. The tail-race water from irrigation dams is another possible field. The hydropower of such barriers is mostly left untapped since it is considered uneconomic to have additional structure just for power generation. Conventional cross-flow turbines are ideal for high velocity-low head applications; yet, a revised upgraded version of cross-flow turbines is necessary for effectively tapping energy from the dam's tailrace primarily meant for irrigation purposes. The complexity(disadvantage) of the vane angle of the cross-flow turbine, as mentioned earlier, is also absent in the modified ones. Gorlov helical turbine (GHT), as shown in Figure 3, is fundamentally an enhanced version of the Darrieus type water turbine, differing mainly in the configuration of blades. The straight vertical vanes of the Darrieus turbine are replaced with helically shaped ones similar to the DNA strands. This increases the possibility of encountering a blade segment with every azimuthal angle of the turbine.

The production of complex geometric aerofoil structures proved to be difficult at those times. These issues no longer exist with improvements in additive manufacturing, such as 3D printing. The prototype uses a three-blade configuration for optimum efficiency, as mentioned in the literature and experiments [9]. The blade profile employed in the simulation and experiment is NACA 4412 with a 0.0228 m chord length. A comparison of the various profiles used for the GHT is illustrated in figure 4. Although it appears that S1210 has the edge over NACA 4412, it is challenging to manufacture.

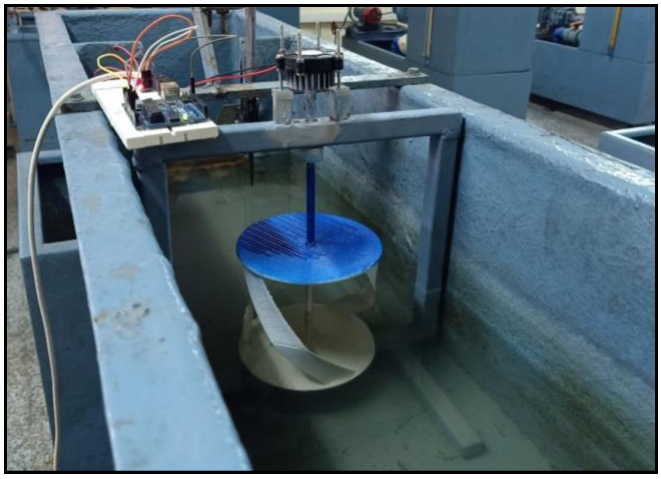

Fig. 3. Gorlov Helical Turbine Installed in a horizontal channel (test bed).

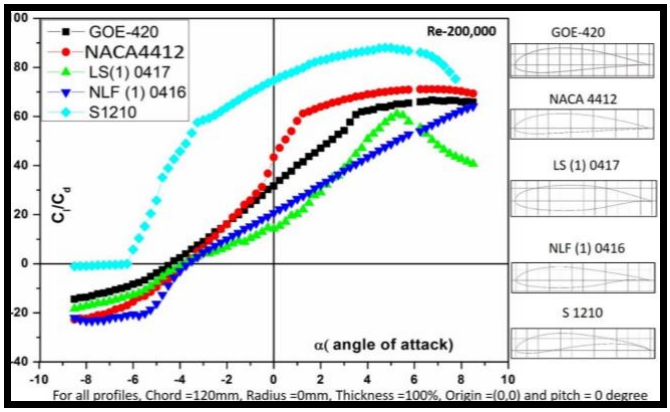

Fig. 4. Comparison of different GHT aerofoil profiles

3. Governing Equations of GHT

The most frequently utilized attribute of a turbine's structure [10] is its relative solidity, which is defined as:

$$\sigma = \frac{nc}{\pi D} \tag{1}$$

where n denotes the number of turbine blades, c represents the chord length of the blades, and D is the turbine's diameter. To calculate the solidity ratio in terms of projected areas (in the vertical plane of the turbine shaft) of the vane, M. Gavasheli developed an equation 2 [8, 10]. Representing the helical turbine's solidity by P (in terms of vane's plan on the lateral plane [8,10]),

$$P = \frac{2nHr}{\pi}\left(d + \sum_{j=1}^{n} Sin\left(\frac{j\pi}{n} - d\right) - sin\left(\frac{j\pi}{n}\right)\right) \tag{2}$$

where H and r are the height and radius of the turbine. Substitute σ = S/2Hr as relative solidity of the turbine in equation 2. Further generalization of the equation involves integrating the value of 'd' in chord (in radians). A three-

blade arrangement was opted owing to self-starting feature, and hence the final expression for relative solidity would be:

$$\sigma = \frac{3}{\pi}\left(d - \sqrt{3} + Sin(d) - \sqrt{3}Cos(d)\right) \quad (3)$$

Furthermore, the following formula is used to determine the tangential force on the turbine:

$$F = \frac{1}{2} C_d \rho \sigma A V^2 \quad (4)$$

C_d is the drag coefficient, ρ is the density of fluid (1000 kg/m^3), A is the projected frontal area, V is the velocity of the fluid. The force is owing to the pressure exerted by the dynamic fluid on the projected area assessed with the aid of solidity ratio (relative). The torque shall be calculated accordingly:

$$T = F \times r \quad (5)$$

The output power of the GHT can be assessed using the idealistic formula

$$P = T \times \omega \quad (6)$$

The Tip Speed Ratio can be calculated as:

$$\lambda = \frac{\omega D}{2 V} \quad (7)$$

where ω is the angular velocity of the turbine.

In addition to TSR, coefficient of power (C_p) [10,11] is often employed to evaluate the performance of turbine.

$$C_p = \frac{T\omega}{\frac{1}{2}\rho\sigma A V^3} \quad (8)$$

Equation (1) to (8) are adapted from the previous research article published in terms of index of revolution [10]. The operating conditions of the turbine are briefed in Table 1.

Table 1. Operational conditions of GHT

Nomenclature of turbine	Vertical axis cross flow hydro turbine (Helical blades)- GHT
Class (power)	Micro turbine
Diameter and height of the turbine	0.130 m × 0.135 m
Profile of blade	NACA 4412
Chord length	0.0228 m
Centre of gravity	(0.0573,0.1033, -0.0067) m
Mass and Moment of inertia	0.15 kg, 0.0016 kg/m^2
Velocity of water	2.54 m/s

4. Simulation of GHT using Dynamic Mesh with 6 DOF (Degree of Freedom) in Ansys Fluent

The dimensions of the computational domain are 0.262 m x 0.275 m x 0.750 m (Width, Height, Length). The computational domain is illustrated in Figure 5. The inner cylinder has a diameter of 0.175 m, which facilitates the dynamic mesh. The turbine axis was held 0.05 m from the inner sidewall of the duct to reduce the influence of wake and turbulence. The turbine was placed 0.1625 m from the inlet section (longitudinal direction). The SI system was used for all calculations. All parameters employed for simulations are detailed in Table 2.

Table 2. Parameters employed in the simulation

Parameter	Value
Dimension of turbine	0.130 m × 0.135 m
Computation Domain	0.262 m x 0.275 m x 0.750 m
Density of fluid	1000 Kg/m^3
Fluid velocity	2.54 m/s
Boundary conditions- Front Face	Velocity opening
Boundary conditions- Rare Face	Pressure opening
Left, Right and Bottom &Top face	No slip
Turbulence model	K-ε Model
Scheme	SIMPLE pressure-velocity coupling method with second order upwind scheme
Mesh size	7.3315 x10^{-12} m (Min), 1.705 x10^{-6} m (Max), 2.767 x 10^{-9} m (Avg)
Y^+ (Dimensionless distance of first cell height to the wall) wall	0.98

In this simulation [12], the Ansys Work bench's Dynamic mesh with 6 DOF approach was used. Dynamic meshing [13] enables the inclusion of moving components without resorting to overset meshing. Hence the errors due to interpolation at the component or background interface can be eliminated. Another advantage is that the feature detects gaps in the wall-to-wall contacts and prevents fluid leakage.

Good use of dynamic meshing is in the rigid body motion, which involves the movement of boundaries or internal walls relative to one another. The passive solution can be used to specify the motion of the walls using the 6-degree of freedom (6 DOF) solver. This will cause the wall to move according to the forces generated by the fluid. Layering is a particular sort of dynamic mesh. This approach utilizes hex or prism cells to eliminate an entire section at a time. Layering obviates the need for sophisticated re-meshing techniques, making it highly robust. Dynamic meshing enables CFD to model a broader spectrum of fluid flow applications without regard for wall boundaries.

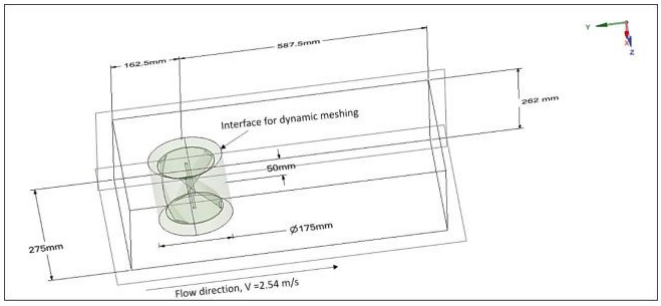

Fig. 5. Layout of computational domain.

The type of study was labelled as "internal" (internal flow). As the flow was parallel to the Y-axis, all other orthogonal gravity elements were set to zero, except for the Z-axis. The rotational field was marked as local. Water was chosen under the fluid domain. Solidworks was used for drafting the model, and then the geometry was imported to the Ansys workbench. In design modular, all possible model editing is compiled. The outer and inner domains were then defined, and the computational domain field was determined using an appropriate Boolean. The outlet and inlet gates were then specified, with the inlet being driven by velocity as mentioned in Table 2 and the outlet by pressure. After that, the geometry was imported into Fluent for meshing. Local sizing is essential because of the fluid interaction. The growth rate in local sizing was set as 1.2. The minimum, maximum and average mesh sizes are 7.3315 x10^{-12} m, 1.705 x10^{-6} m, and 2.767 x10^{-9} m, respectively. The geometry has 2,851,495 nodes. Details of the mesh are illustrated in Figure 6.

For dynamic meshing, a steady-state model is chosen. The number of iterations was marked as 2000. Various turbulence models are accessible within Ansys Fluent to address the influence of turbulence in numerical research. The modified k-ε turbulence (using Favre-averaging) model has been the prevalent choice in our previous research [14] for modelling turbulence. Indeed, prior investigations [12,14,17] indicated that the k-ε turbulence model [15-17] is more effective in simulating fluid through rotating aerofoils or blades as well as flows with separation or boundary layer effects. Consequently, we have verified that the k-ε model is the most appropriate choice for simulating a hydrokinetic turbine. At the inlet section, the fluid velocity was set to 2.54 m/s in the boundary condition. Layering and re-meshing are used to smoothen the dynamic models. The mesh was tetrahedral in form. The centre of gravity, mass and moment of inertia was specified in the 6 DOF menu settings as mentioned in table 1. Both external and internal domains are then introduced. The required set of data points were selected before initialization. Setting time steps is essential and fixed based on iterations. The geometric was mentioned as a mix of fluid and solid regions with shear topology [16]. For each iteration, the convergence necessities for all residual formulations of continuity, momentum, and performance Chara's are defined as 10^{-3}. The characteristics of the angular velocity acquired for each time step [16] are listed in Table 3.

Table 3. Flow conditions

Reynolds number	Simulation time step	Angular velocity	TSR
21.01 x 10^4	0.000354	6.80	0.18
	0.000708	7.22	0.19
	0.00107	7.33	0.19
	0.001436	8.06	0.21
	0.001831	12.56	0.33
	0.002237	16.75	0.44
	0.002649	19.36	0.50
	0.003083	23.03	0.60
	0.00353	25.54	0.66
	0.003995	26.17	0.68
	0.004469	28.89	0.75

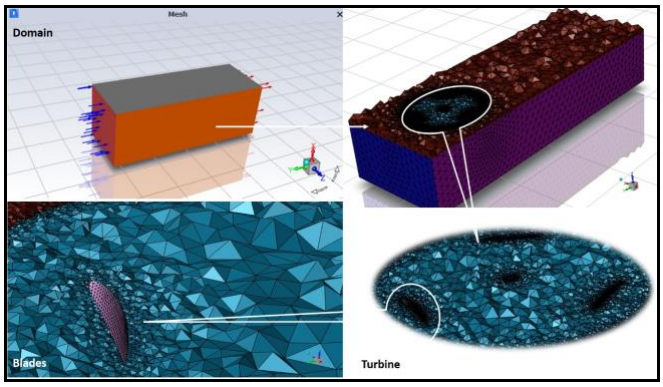

Fig. 6. Mesh details of computational domain

The meshed model consists of three primary zones: the exterior region, the rotating region, and the area in proximity to the helical blades. The rotating region employs a fine mesh, while the exterior region utilizes a coarse mesh. Tetrahedra, also referred to as simplexes, have the unique characteristic of being able to mesh any 3D volume, regardless of its shape or topology. Additionally, they are the

sole element type compatible with adaptive mesh refinement. Therefore, the tetrahedral mesh was chosen for the study. Necessary inflation layers were also provided to preserve the geometry from distortion.

The impact of varying the number of mesh elements on the power coefficient was examined in a mesh independence study using ANSYS, with a flow velocity of 2.54 m/s. Six different mesh models denoted as M1 to M6, were included in this study, having element counts of 2,386,922, 2,500,109, 2,697,990, 2,752,500, 2,851,495, and 2,954,550. A graph (Figure 7) illustrates the relationship between the power coefficient and the number of mesh elements. To estimate the error, a predetermined value of C_p=0.2463, as found in the literature, was utilized. Notably, there were no significant enhancements in the power coefficient observed when the number of mesh elements exceeded 2,851,495 (M5). Consequently, for efficiency reasons, mesh model M5 was selected for subsequent simulation studies.

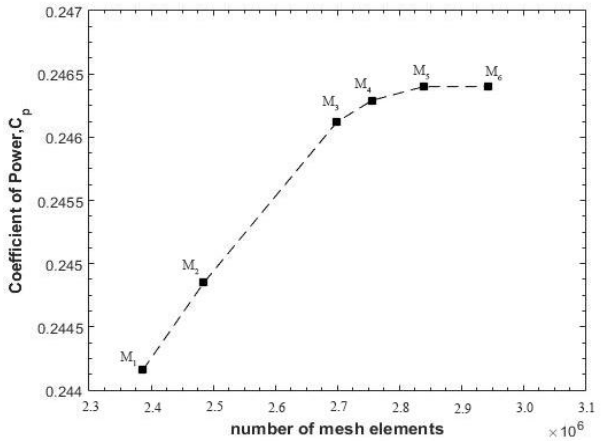

Fig. 7. Mesh independency: C_p Vs number of elements

5. 3D Printing for Prototype Development (GHT)

The FlashForge 2.0 finder is built to handle complex structures. The machine uses the principle of tomography for "printing" the prototype [18]. The slide-in construction plate (built plate) and assisted bed levelling are novel features that researchers appreciate for their quiet and safe operation. The heated components are carefully encased in the finder, which is made entirely of PLA. The maximum print volume is limited to 140 x 140 x 140 mm^3. The layer resolution varies within 0.4mm. The rated voltage and current are 100-240 V/2.7 A with a power rating of 60 W. The maximum tip speed is 100 mm/s. A 1.75 mm premium-quality 3D Filament of PLA (Polylactic acid) is employed to ensure flawless feeding and extrusion. PLA is the standard suggested material for 3D printers, and for a good goal: it works well in a wide range of applications, is fragrance-free and low-warp, and does not necessitate a heated platform. Due to the complexity of the model, SolidWorks was used to draft the model. Then the file was saved in stereo lithography format (.stl file) on the SD card, which can be inserted in Flash Forge Finder. The user can scale the part drawing to the correct size using the Flash print software. Slicing, dimensional correction, and choosing the type of support for the prototype are all done with Flash print. The G-code and M-codes necessary for the machine are generated using the flash print software. figure 8 illustrates the different stages of 3D printing the prototype.

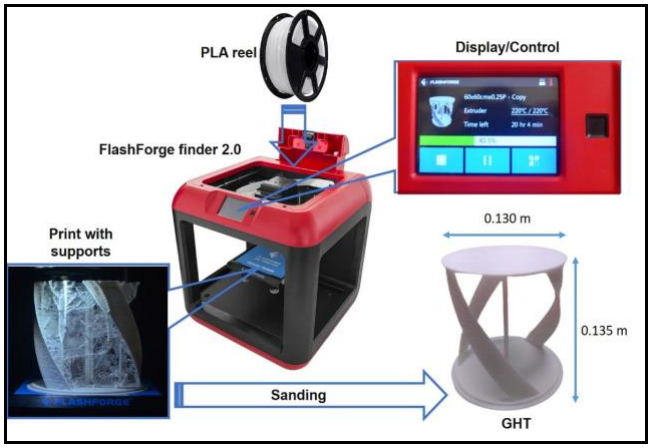

Fig. 8. Different stages of 3D printing the prototype

6. Experimentation

The turbine prototype had the same height and diameter as the simulated model, with an aspect ratio of almost a unit. The chord length of the prototype was 0.0228 m. It has been already proved in our previous studies [14,17] that the optimum index of revolution was 0.25 and hence this value was used. Since Unsymmetrical aerofoils are known to enhance the turbine's performance in low-velocity streams [19], NACA 4412 was selected as the blade's profile. The GHT was housed in a towing tank with a rectangular cross-section (0.290 m wide x 0.295 m deep) and 1.180 m in length. A mount is installed towards the towing tank's end, where a triangle or rectangular notch can be attached [10]. This is used to determine the flow velocity. There are two collecting tanks held side by side in addition to the rectangular towing tank. Water is pumped from the reservoir to the first collecting tank, from where it progressively moves towards the rectangular tow tank. A set of strainers were used to control the flow's turbulence. The GHT was housed in a rectangular structural frame using bushes rather instead of than bearings. The structure was designed to slide into the rectangular channel easily. An Xcluma-built 5V/ 10W DC micro-hydro generator was installed on the rotational axis of GHT using bushes. Throughout the experiment, a constant head of 0.2m was maintained at a velocity of 2.54 m/s. The configurations are depicted in Figure 9.

The measurement of voltage and current from the microgenerator involves instrumentation, as illustrated in Figure 10. Simultaneous measurement of these parameters at the milli-scale is always challenging. The instrumentation involves an Arduino Uno board, Ammeter (ACS721), 100 Ohm Resistor and Microturbine (Xcluma-built). The rotational motion of GHT is converted into voltage and current utilizing the microturbine. The Arduino is an open microcontroller board designed by Arduino Corporation and based on the ATmega328P microprocessor.

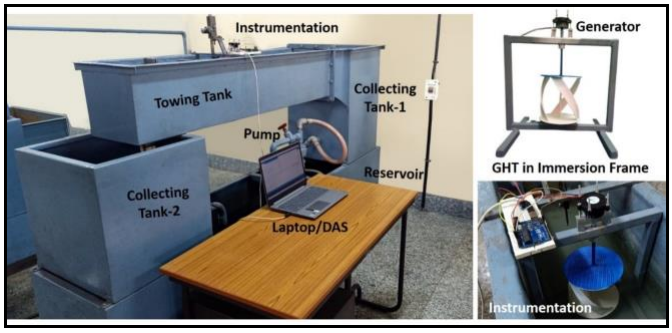

Fig. 9. Experiment setup.

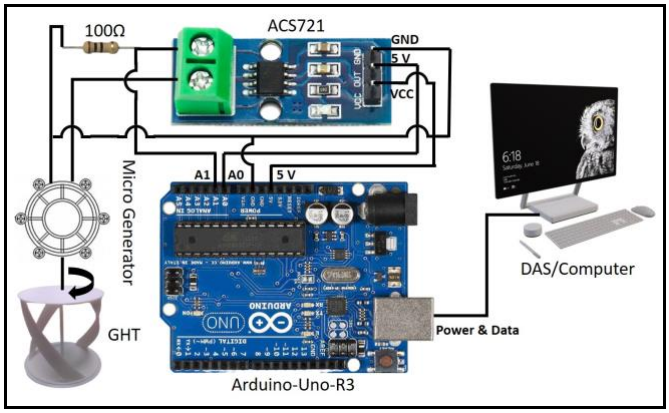

Fig. 10. Circuit diagram for current and voltage measurement.

The board has several digital and analogue output/input ports connected to dissimilar expansion boards and other circuits. The board features 14 digital input/output pins (six of which are capable of Pulse width modulation output), six analogue input/output pins. It is programmable through a type B USB cable using the Arduino Integrated Development Environment. The board is powered using a USB cable connected to the laptop. The boarded hall sensor circuit in the ACS712 is used to detect current. The magnetic field of the hall effect sensor perceives the incoming current. The hall effect sensor generates a voltage equivalent to the magnetic field once the ammeter detects it. The Arduino board measures this voltage. A code that converts the measured voltage into the current is compiled and uploaded (Flashed) to the microcontroller. The formula for the above-mentioned is:

$$I = (2.5 - (V/0.185)) \quad (9)$$

A 5V battery was connected in series with a 220-ohm resistor and LED bulb. To calibrate the Arduino, voltage and current readings across the LED bulb were measured using a standard Multimeter. These readings were then compared with the output of the program from Arduino. The results were satisfactory and values were within standards [20]

7. Uncertainty Analysis

The output power is calculated as the product of the current and voltage developed by the Xcluma-built mini generator. Equation 10 was used to compute the uncertainty. The equation was tailored using Moffat's approach [21], and the deviation (in output power) was 1.24%.

$$\frac{\partial P}{P} = \left[\left(\frac{\partial v}{v}\right)^2 + \left(\frac{\partial I}{I}\right)^2\right]^{\frac{1}{2}} \quad (10)$$

In equation 10: P, V, and I denote output power, Voltage and Current, respectively. Table 4 summarizes the systematic error allied with the countable measuring equipment evaluated in this investigation. The error levels and uncertainties were all within tolerable limits.

Table 4. Systematic error of gauging instruments

Gauging instruments	Systematic error
ACS712 (for current measurement)	0.26 %
Xcluma Micro Generator	2.26 %
Digital tachometer (laser-based, non-contact)	3 %

8. Results and Discussion

Figure 11 and 12 illustrates the dynamic pressure and total pressure of the GHT. The pressure variation is plotted in the ZY midplane. Variation of pressure values is visible along the cross-section of the blades. Steady-state convergence is obtained in the 1027th Iteration.

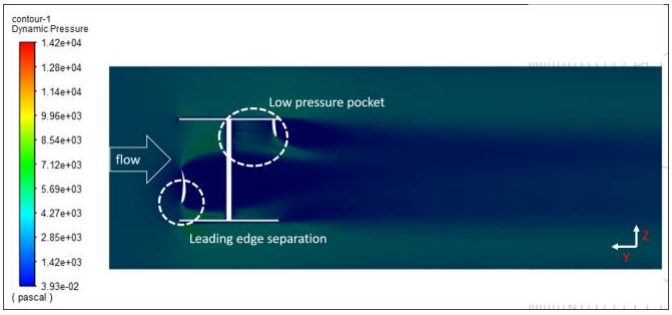

Fig. 11. Dynamic pressure plot for GHT.

Figure 13 denotes the velocity contour of the GHT. The Fluid analysis of GTH on streamlines provides gripping pressure and velocity patterns. The general pressure pattern is such that the gradient of pressure at the centre of the vanes is more than that on the disc edge. This owes to the fact that blades oppose the maximum area (projected) against the flow. The pressure pattern highlights the need for stiffening at the mid-point of blades while fabricating larger turbines. Figure 14 denotes the velocity streamline contour of the GHT model. The streamlines are uniform, and the effect of wake and local rotation is absent. The power coefficient and output power are plotted concerning the tip-speed ratio in Figures 15 and 16. As a result of these findings, it is clear that the power coefficient improves with the TSR, eventually reaching a value of 0.113. When the turbine's rotation

velocity is 28.8 rad/s, the power coefficient reaches a maximum value.

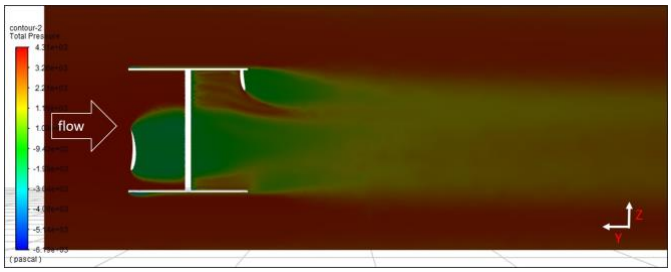

Fig. 12. Total pressure plot for GHT.

Fig. 13. Velocity plot for GHT

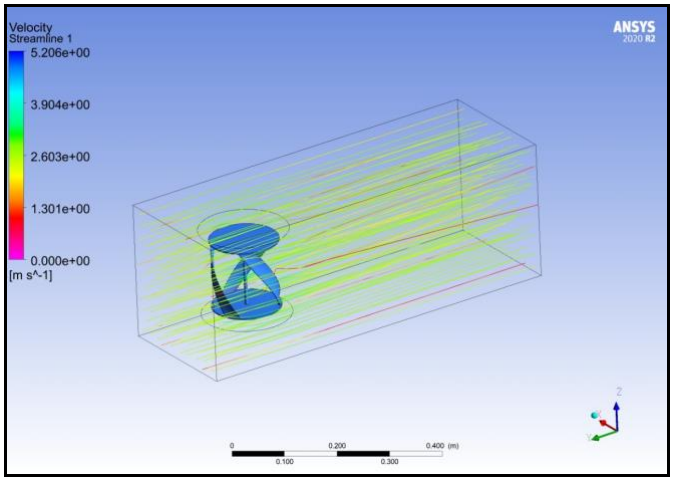

Fig. 14. Velocity stream line contour of GHT

However, the plot variation is independent of the loading effect of the micro-generator. The output power tends to rise with the TSR in the output power Vs the TSR plot. The maximum output power is 2.95 W for a TSR value of 0.751. The general trend for C_p Vs TSR first increases and reaches saturation, followed by depreciation [14]. However, only the first leg is visible in Figure 15, as the value of TSR is limited by 0.8. Table 5 illustrates the experimentation data from the 3D printed turbine. The Monoblock pump supplies water to collecting tank 1, as presented in Figure 9. The strainers located in the tank help to remove the turbulence of the water. The water then moves towards the towing section of the apparatus. The flow velocity is controlled by the butterfly valve located in the delivery pipe. This velocity is further confirmed by the triangular notch located at the end of the tow tank. The notch also helps to maintain a head for the turbine. The generator connected to the turbine shaft starts rotating with the flow. The Data Acquisition console system records the voltage and current (in the current research - a computer). Table 5 illustrates the data from the generator attached to the system. Steady-state in terms of reading is achieved shortly after the commencement of flow. The output power of the turbine was noted as 1.248 W for a constant velocity of 2.54 m/s.

Fig. 15. Variation of Cp (coefficient of power) with respect to TSR

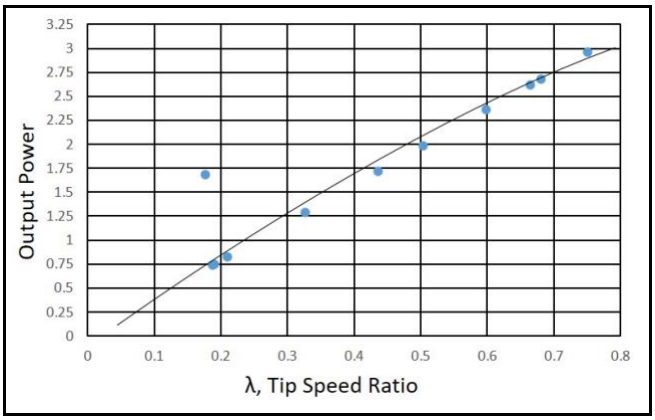

Fig. 16. Variation of output power with respect to TSR

Table 5. Experimental results

Time step (S)	Current (A)	voltage (V)	Power (W)
1	0.41	2.24	0.9184
2	0.44	2.24	0.9856
3	0.46	2.25	1.035
4	0.47	2.27	1.0669
5	0.53	2.24	1.1872
6	0.53	2.25	1.1925
7	0.53	2.27	1.2031

8	0.53	2.23	1.1819
9	0.56	2.23	1.2488

Table 6. Comparison of simulation and experimentation results of GHT

Index of revolution	Fluent simulation result	Experimentation result
0.25	1.78 W	1.24 W

A GHT was drafted using Solidworks and analysed using the fluid simulation module Fluent in Ansys workbench. The inlet velocity was 2.5 m/s. The output power as per simulation was 1.78 W. A prototype model was printed using 3D printing and experimentally validated against simulation. The output power developed by the turbine in the experiment was 1.24 W. Table 6 draws a comparison of the simulation and experimentation. The experimental value is less than the simulation as expected. The mechanical loss and excess circulation in the flow field would be the reason for the mismatch. Best efforts were chosen to control the wake and turbulence. However, over the period, these disturbances will make through the system. The geometry of the turbine used in the current research is similar to that of Valdés [22]. It is observed from Valdés [22] experiment that the peak power of GHT at 270 Rpm was around 0.8 W to 1.0 W for a velocity of 0.60 m/s to 0.65 m/s. However, for a lower rpm (230 rpm) Valdés [22] managed to clock 5 W. These results serve as a bench mark for the current research and emphasis the room for improvement.

9. Conclusions

The Government of India began its efforts to set up mini-off grids back in 2015. However, in 2018-19, the need to integrate electricity from renewable sources and mini off grids to the national power grid was realized. The studies recommend a viable solution by using unexploited potentials such as the tailrace/runoff water for India's struggling small hydropower units. The purpose of this study was to determine whether a cross-flow turbine would be suitable for generating electricity from a dam's tailrace. To accomplish this goal, steady-state three-dimensional turbulent flow simulations on a vertical axis cross-flow turbine with helical blades (GHT) were conducted. Ansys Fluent was used for analysis and post-processing. A velocity of 2.54 m/s was applied to a GHT model to mimic the field conditions. A relatively new yet highly effective technique called dynamic meshing with six degrees of freedom was applied. Following that, the model was 3D printed and subjected to comparable circumstances. The turbine's performance was evaluated using the Cp and output power versus the tip speed ratio and was adequate. As a result, it can be stated that Gorlov Helical turbines can be used to generate electricity from in the dam's tailrace, thus enhancing the grid capacity [23,24,25] of SHPs.

10. Limitation of System

•The surface smoothness of the helical blade could be improved using an ABS (acrylonitrile butadiene styrene) reel-in 3D printer.

•Optimising the chord length of the turbine will result in better efficiency

•The blockage effect on the turbine was not studied.

Acknowledgements

The authors of the paper are thankful to the Kerala Water Authority and Er Vishnu C.S (Asst. Engineer, KWA) for providing the necessary data on the Aruvikkara dam.

Nomenclature

σ Relative solidity

n Denotes the number of blades

b Chord of each blade cross-section, m.

D Diameter of the turbine, m.

H Height of the turbine, m.

r Radius of the turbine, m.

d Half of the blade's chord in radians with respect to

the axis of rotation, rad

$\mathbf{C_d}$ Coefficient of drag as per NACA

$\mathbf{C_p}$ Coefficient of power

V, I Voltage, (V) and Current (A)

λ Tip speed ratio (TSR)

References

[1] M. Khan, M. Iqbal, and J. Quaicoe, "River current energy conversion systems: Progress, prospects, and challenges," Renewable and Sustainable Energy Reviews, vol. 12, no. 8, pp. 2177–2193, 2008.

[2] A. M. Gorlov, "Helical turbines for the Gulf Stream: Conceptual approach to design of a large-scale floating power farm," Marine Technology and SNAME News, vol. 35, no. 03, pp. 175–182, 1998.

[3] M. Shiono, K. Suzuki, and S. Kiho, "Output characteristics of Darrieus water turbine with helical blades for tidal current generations," 12th International Offshore and Polar Engineering Conference, Kitakyushu, Japan, pp. 859–864, 26-31 May 2002.

[4] S. Pongduang, C. Kayankannavee, and Y. Tiaple, "Experimental investigation of helical tidal turbine characteristics with different twists," Energy Procedia, vol. 79, pp. 409–414, 2015.

[5] Y. Liu and D. J. Packey, "Combined-cycle hydropower systems – The potential of applying hydrokinetic turbines in the tailwaters of existing conventional hydropower stations," Renewable Energy, vol. 66, pp. 228–231, 2014.

[6] E. Quaranta and S. Muntean, "Wasted and excess energy in the hydropower sector: A European assessment of tailrace hydrokinetic potential, degassing-methane capture, and waste-heat recovery," Applied Energy, vol. 329, Article 120213, 2023.

[7] M. A. Arango, "Resource assessment and feasibility study for use of hydrokinetic turbines in the tailwaters of the Priest Rapids Project," Thesis, University of Washington, 2011.

[8] A. M. Gorlov, "The helical turbine and its applications for hydropower without dams," Advanced Energy Systems, Proceedings of IMECE2002 ASME International Mechanical Engineering Congress & Exposition, New Orleans, Louisiana, pp. 257-264, November 17-22, 2002.

[9] P. K. Talukdar, V. Kulkarni, and U. K. Saha, "Field-testing of model helical-bladed hydrokinetic turbines for small-scale power generation," Renewable Energy, vol.127, pp. 158–167, 2018.

[10] V. Jayaram and B. Bavanish, "A brief review on the Gorlov helical turbine and its possible impact on power generation in India," Materials Today: Proceedings, vol. 26, no. 5, pp. 156–163, 2020.

[11] B. Bavanish and K. Thyagarajan, "Optimization of power coefficient on a horizontal axis wind turbine using BEM theory," Renewable and Sustainable Energy Reviews, vol. 26, pp. 169–182, 2013.

[12] O. N. C. U. Selim, U. Tuncer, and S. Koyuncu, "Modeling and simulation of external rotor 6/8 switched reluctance motor for e-bike," 10th International Conference on Smart Grid (icSmartGrid), Istanbul, Turkey, pp. 351–355, 2022.

[13] Y. You, S. Wang, W. Lv, Y. Chen, and U. Gross, "A CFD model of frost formation based on dynamic meshes technique via secondary development of ANSYS Fluent," International Journal of Heat and Fluid Flow, vol. 89, pp. 1–8, 2021.

[14] V. Jayaram and B. Bavanish, "A brief study on the implementation of helical cross-flow hydrokinetic turbines for small scale power generation in the Indian SHP sector," International Journal of Renewable Energy Development, vol. 11, no. 3, 2022

[15] S. Galvan, M. Reggio, and F. Guibault, "Assessment study of K-ε turbulence models and near-wall modelling for steady state swirling flow analysis in draft tube using Fluent," Engineering Applications of Computational Fluid Mechanics, vol. 5, no. 4, pp. 459–478, 2011.

[16] M. Mosbahi, A. Ayadi, Y. Chouaibi, Z. Driss, and T. Tucciarelli, "Experimental and numerical investigation of the leading-edge sweep angle effect on the performance of a delta blades hydrokinetic turbine," Renewable Energy, vol. 162, pp. 1087–1103, 2020.

[17] V. Jayaram, B. Bavanish, "Design and analysis of gorlov helical hydro turbine on index of revolution." International Journal of Hydrogen Energy, Vol 47 (77), pp 32804-32821, 2022.

[18] B. Shaqour, M. Abuabiah, S. Abdel-Fattah, A. Juaidi, R. Abdallah, W. Abuzaina, M. Qarout, B. Verleije, and P. Cos, "Gaining a better understanding of the extrusion process in fused filament fabrication 3D printing: A review," International Journal of Advanced Manufacturing Systems, vol. 114, no. 1, pp. 1279–1291, 2021.

[19] G. Saini and R. P. Saini, "A review on technology, configurations, and performance of cross-flow hydrokinetic turbines," International Journal of Energy Research, vol. 43, pp. 6639–6679, 2019.

[20] P. Sanchez-Sutil, G. Cano-Ortega, J. Hernandez, and C. Rus-Casas, "Development and calibration of an open source, low-cost power smart meter prototype for PV household-prosumers," Electronics, vol. 8, no. 8, p. 878, 2019.

[21] R. J. Moffat, "Describing the uncertainties in experimental results," Experimental Thermal and Fluid Science, vol. 1, no. 1, pp. 3–17, 1988.

[22] R. Espina-Valdés, A. Gharib-Yosry, R. Ferraiuolo, A. Fernández-Jiménez, and V. M. Fernández-Pacheco, "Experimental comparison between hydrokinetic turbines: Darrieus vs. Gorlov," Environmental Sciences Proceedings, 5th EWaS International Conference, Naples, Italy, 12–15 July 2022.

[23] S. Goud, T.V. Sai Kalyani, K.V. Govardhan Rao, and G. Sanjeev, "Amalgamation of smart grid with renewable energy sources," International Journal of Smart Grid, vol. 7, no. 2, pp. 103-107, June 2023.

[24] A. Salehpour, I. Al-Anbagi, K.-C. Yow, and X. Cheng, "A Realistic Failure Propagation Model for Smart Grid Networks," 2022 10th International Conference on Smart Grid (icSmartGrid), Istanbul, Turkey, pp. 66-71, 2022.

[25] A. AlKassem and M. AlKabi, "A TOPSIS Model to Support Smart Appliance Decision Energy Management in Smart Grid," 2022 11th International Conference on Renewable Energy Research and Application (ICRERA), Istanbul, Turkey, pp. 534-539, 2022.